Visualization of the flow around a bubble moving in a low viscosity liquid

R. Lima-Ochoterena and R. Zenit*
Instituto de Investigaciones en Materiales, Universidad Nacional Autónoma de México
Apartado Postal 70-360, Cd. Universitaria, México D.F. 04510, México

A new technique to visualize the flow around a bubble rising in a low viscosity fluid is presented. With this technique it is possible to observe streak lines of the flow as well as the shape and position of the bubble. The visualization of the streak lines is obtained by open-diaphragm photography of laser-sheet illuminated micro-tracers. The shape and position of the bubble is obtained, in the same photo plate, by simultaneously illuminating the flow with a stroboscopic light. The experiments were performed in a closed acrilic tank of $50 \times 50 \times 50$ cm^3, in which bubbles were injected using a capillary tube. Filtered water was used as the working fluid. Pure Nitrogen was used to form the bubbles. Experimental results were obtained for a range of bubble sizes. The size of the injected bubbles was controlled by a fixed volume switch valve. We have identified a change of the bubble trajectory, from rectilinear to zig-zaging, as its volume increases, in accordance with previously reported studies. A characteristic change of the velocity field around the bubble is observed when the trajectory instability appears. We conclude that the point of inflection in the velocity-volume plot is directly related to the appearance of the trajectory instability.

Keywords: Bubbles; terminal velocity; path instability; flow visualization.

Presentamos una técnica para la visualización del flujo alrededor de una burbuja que se mueve en un líquido newtoniano de baja viscosidad. Esta técnica nos permite observar las líneas de corriente, así como la forma y posición de la burbuja de manera simultánea. La visualización de las líneas de corriente se logra a través de la fotografía por obturador abierto de micro-partículas trazadoras iluminadas por una hoja láser. La forma y la posición de la burbuja se captan en la misma impresión fotográfica iluminando al flujo, de manera simultanea, con una lámpara estroboscópica. Los experimentos se realizaron en un tanque cerrado de $50 \times 50 \times 50$ cm^3, en el cual se inyectaron las burbujas a través de un capilar. Se utilizó agua filtrada y nitrógeno puro para formar las burbujas. Obtuvimos resultados experimentales para el flujo de burbujas de diferentes tamaños. El tamaño de las burbujas se controló, para un mismo capilar, con una válvula de conmutación de volumen constante. Con estas mediciones se identificó la transición de trayectoria, de rectilínea a oscilatoria, para una burbuja en agua, de manera similar a lo reportado con anterioridad en la literatura. La aparición del cambio en la trayectoria está asociada con un cambio importante de la estructura del flujo alrededor de la burbuja. Además, obtuvimos una correlación del punto de inflexión de la curva velocidad-volumen con la aparición de la inestabilidad de trayectoria.

Descriptores: Burbujas; velocidad terminal; inestabilidad de trayectoria; visualización.

PACS: 47.55.Dz; 47.20.Ky; 47.20.Ft; 47.55.Kf

1. Introduction

The study of the fluid motion around immersed objects has played a significant role on the development of modern fluid dynamics. In particular, the motion of bubbles in liquids have captured the attention of scientists for many years. This apparently simple problem has many practical applications [1, 2] and is also of fundamental importance for the proper characterization of gas-liquid flows [3].

The motion of bubbles in different liquids has been studied extensively for decades [4]. Many experiments have demonstrated that millimetric size rising bubbles do not follow a straight trajectory. In pure water, bubbles of ellipsoidal shape transition from a straight to a zig-zag trajectory for sizes larger than 1.8 mm [5]. Many studies have found that surface impurities produce significant changes in the behavior of these systems; even tiny amounts of contaminants cause the transition to appear at much smaller sizes. The stability problem has been studied both experimentally and theoretically (see Refs. [6] and [7] for recent accounts). There is still a lack of general agreement on the fundamental mechanisms that trigger the transition.

The value of the bubble terminal velocity has been also obtained by many investigators [4]. For air-water systems, it is generally agreed that the velocity increases monotonically with bubble size up to a size of approximately 1.6 mm. For bubbles of a larger size, the velocity does not continue to increase. It remains relatively constant for a certain size range, and eventually, continues to increase for larger bubble sizes. Results obtained for Nitrogen bubbles in ultra-pure water [5] are in agreement with theoretical predictions based on potential flow assumptions [8]. However, contamination in the gas-liquid interface has also a significant effect on the value of the terminal velocity and the appearance of the plateau in the velocity curve. It is not clear whether the inflection point on the velocity-size curve is related to the appearance of the oscillatory nature of the trajectory. Moreover, recent investigations [6] have shown that the terminal velocity and the shape are also affected by the formation process of the bubble.

We consider that in order to further improve the general understanding of the transition to an oscillating trajectory and its relation to the bubble terminal velocity and shape, the flow field around the rising bubbles has to be studied. In this paper a new technique to visualize the flow generated by rising

bubbles is presented. Previous attempts to visualize the flow have been limited to a 2-D configuration [9].

2. Experimental setup

The experiments were performed in a square closed tank of $50 \times 50 \times 50$ cm^3, shown schematically in Fig. 1. The walls were fabricated with transparent acrylic sheets of a thickness of 13 mm. The tank was filled with filtered tap water. The water was filtered several times using an recirculation loop that had a dual filtering device. The first filter, an activated carbon column, was used to eliminate organic compounds. To eliminate dust and particulate matter a cloth filter, with a mesh size of 1 μm, was used. Pure Nitrogen was used to form bubbles that were injected through a 1 mm inner diameter stainless steel capillary centered at the bottom of the tank. To vary the size of the bubble to be injected, we used a micro-volume commutation valve (VICI model C14WEE.06) similar to that used in Ref. 5. This valve has a fixed volume chamber that can be filled with a gas and commuted into a liquid stream. The fixed volume is then transported by a small liquid current until it is gently pushed through the capillary and into the tank. The size of the bubble to be released in the tank can be changed by changing the pressure at which the Nitrogen is injected in the fixed volume. With this technique it is not necessary to change the size of the capillary to form bubbles of different diameters.

A first set of experiments was performed to determine the terminal velocity of Nitrogen bubbles in water. The motion of the bubbles was captured using a high speed camera (Kodak Motion Corder 1000) capable to record up to 1000 frames per second. To achieve a proper magnification of the bubble size a Nikkor 105mm Macro 2.8D lens was used. Indirect and diffuse light was used to ensure a good contrast of the bubble with the background. Once the motion of the bubbles was obtained, the images were transferred into a computer using

a frame grabber (EPIX Inc. card). The individual digitized images showed the bubble in different positions, shifted in time. In order to calculate the bubble velocity, the displacement of the geometric center of the bubble images between the consecutive frames was calculated using a computer software (PIXCI SV4). By knowing the frame rate and the displacement of the bubble, the velocity was calculated. Figure 2 shows a typical sequence of digitized images at different positions.
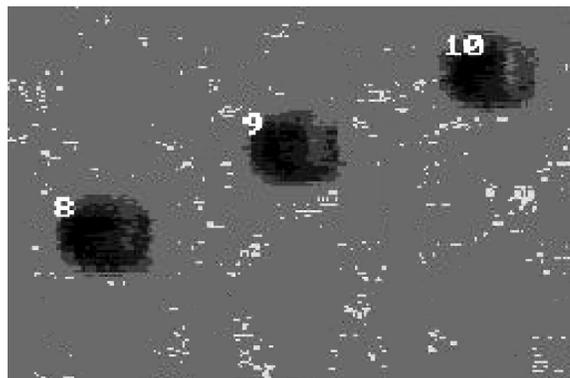
FIGURE 2. Example of digitized bubbles images in a sequence.

2.1. Flow visualization

The main objective of this investigation is to visualize the flow around the bubble and, in a simultaneous manner, observe the shape and size of the bubble. With common techniques it is normally not possible to obtain these two images simultaneously. We propose a new technique to achieve this goal.

The experimental arrangement is shown in Fig. 3. The flow field around the bubble was visualized with the aid of nearly-neutrally buoyant microspheres. The tracers used were silver-coated 10μm hollow glass spheres. These were illuminated with a thin red laser sheet. The laser sheet was produced with a He-Ne laser (Metrologic, Class IIIb, 20 mW), that had a cylindrical lens. To obtain streak lines of the flow

FIGURE 1. Schematic of experimental setup.
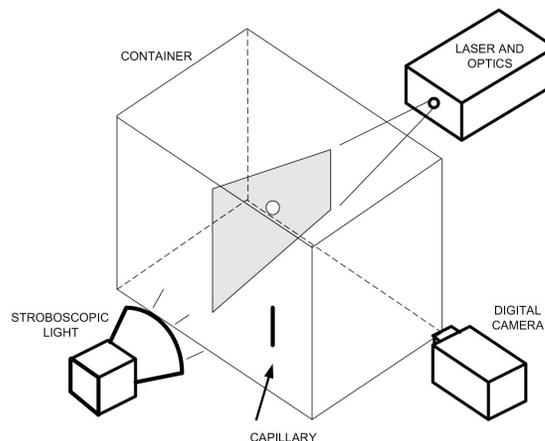
FIGURE 3. Details of the visualization setup.

open diaphragm photography was used. At the moment when the bubble passed through the field of view, the diaphragm of a digital camera (Fuji SIPro, 6Mpixels) was opened. It was kept opened for approximately one second to capture the motion of the tracers. These images had to be captured in a dark environment. The lens used in the camera was a Nikkor 105mm Macro 2.8D. Simultaneously, the flow was illuminated with a stroboscopic lamp. The light emitted by this lamp was intense but of very short duration (less than $50\mu s$). Since the experimental environment was dark, the light from the lamp was reflected only by the gas-liquid interface at the bubble surface; hence, the shape of the bubble could be observed. The flashing frequency of the lamp was controlled by a signal generator (HP 33120A). By increasing the number of flashes per unit time, the shape and position of the bubble could be captured in different positions within the same photographic plate. Bubble images appeared superposed on the flow streak lines. Figures 4 to 7 show examples of the photographs obtained with this technique. These results will be discussed in the next section.

3. Results

The first set of experiments was conducted to measure the terminal bubble velocity as a function of the bubble size, and to determine whether or not the path instability occurred for our experimental conditions. Once these measurements were obtained, experiments were conducted to observe flow fields around bubbles before and after the path instability.

The dimensionless groups that are relevant for this flow are the Reynolds number and the Weber number. The Reynolds number is defined as

$$Re = \frac{U_b D_{eq}\rho_f}{\mu_f}, \tag{1}$$

where U_b is the mean bubble velocity, D_{eq} is the bubble equivalent diameter (defined below) and μ_f and ρ_f are the viscosity and density of the liquid. A large Reynolds number denotes that inertial effects are more important than viscous ones. The Weber number is defined as

$$We = \frac{\rho_f U_b^2 D_{eq}}{\sigma}, \tag{2}$$

where σ is the surface tension of the liquid-gas interface. A small Weber number denotes the dominance of surface tension effects over inertial effects. The shape of bubbles with a small Weber number is closer to spherical.

3.1. Bubble velocity

Since only a plane image of the ellipsoidal bubbles can be obtained through photography, a proper measure of the bubble size has to be defined. The bubble equivalent diameter, D_{eq}, is calculated as,
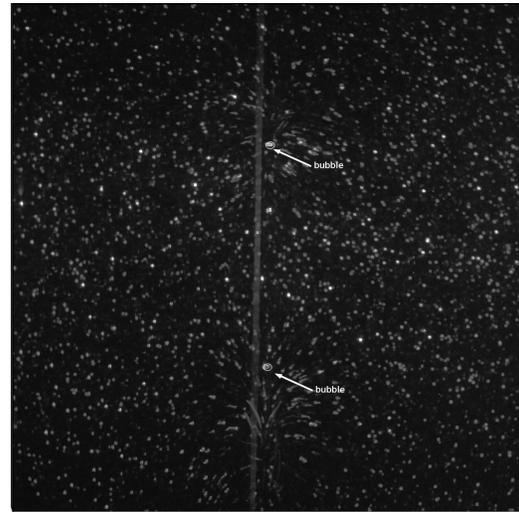
FIGURE 4. Visualization of the flow around a 1.17 mm bubble; Re=140, We=0.25.
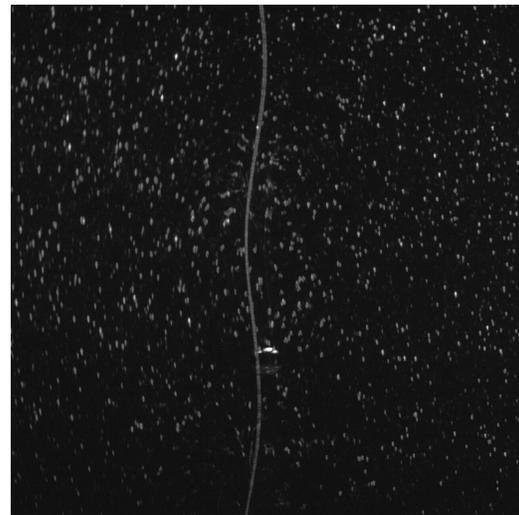
FIGURE 5. Visualization of the flow around a 1.47 mm bubble ; Re=230, We=0.51.
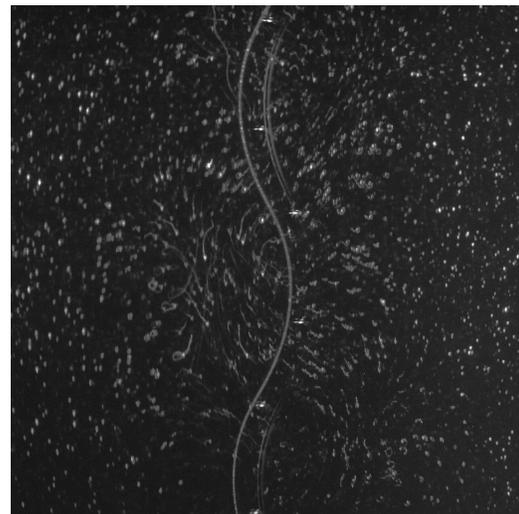
FIGURE 6. Visualization of the flow around a 1.93 mm bubble; Re=320, We=0.73.

$$D_{eq} = (D_{long}^2 \times D_{short})^{1/3}, \qquad (3)$$

where D_{long} is the long axis length of the oblate bubble and D_{short} is the short axis length. For this measurement it is assumed that the bubble is axisymmetric with respect to its short axis direction.
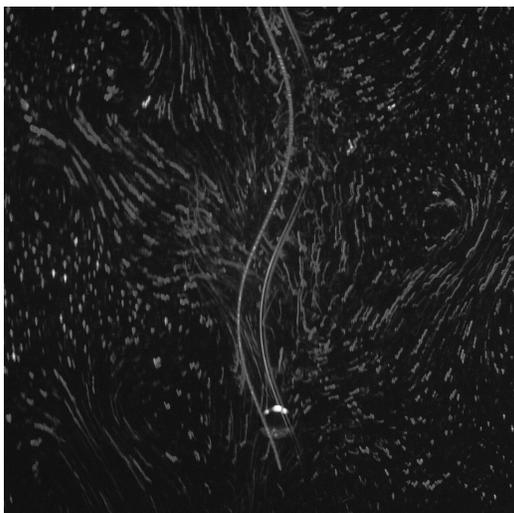
FIGURE 7. Visualization of the flow around a 2.13 mm bubble; Re=364, We=0.89.

Figure 8 shows the mean vertical and horizontal bubble velocities as a function of the bubble equivalent diameter. Each data point was calculated from a single experiment and it is the result of averaging the velocities obtained from each image pair. For each point, a minimum of 30 image pairs was used. For the case of the horizontal velocity, the average is obtained considering the absolute value of the measurement.

For bubbles smaller than 1.6 mm, the vertical velocity increases monotonically and the horizontal velocity is practically zero. For this size range, the trajectory of the ascending bubbles is rectilinear. At approximately 1.65 mm, a point of inflection is observed in the velocity-size curve. Beyond
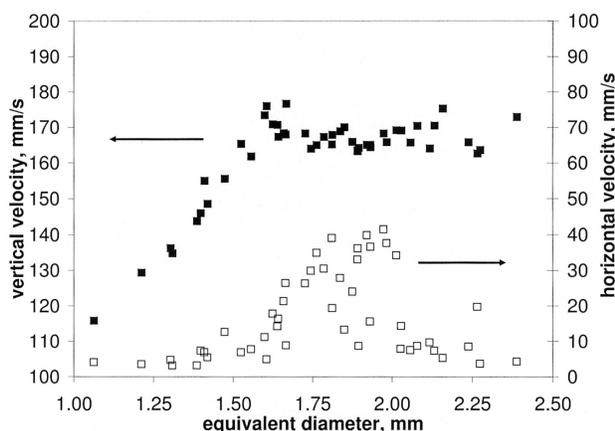
FIGURE 8. Bubble velocity as a function of bubble size.

this point the vertical bubble velocity ceases to increase and remains rather constant despite the fact that the size, hence the buoyancy, increases. At the same point, the mean absolute value of the horizontal velocity increases suddenly. The increase of the horizontal velocity indicates that the bubble is no longer moving is a straight trajectory. The oscillations increase both in amplitude and frequency as the bubble size keeps increasing. The spread observed in the data in this size range depicts the unsteady nature of the flow. The magnitude of the measured vertical velocity is smaller than that reported for pure water [5]. Although our system cannot eliminate all the impurities in the liquid, we do observe the appearance of the inflection point is which has been associated with clean Nitrogen-water systems [4]. The difference found may arise from the 'gentle push' injection technique used in this study. A recent investigation [6] showed that bubbles in ultra clean liquids can have smaller velocities if these are injected into the tank by the 'gentle push' technique.

The transition from rectilinear to oscillatory trajectory appears for the present experimental conditions. Using the proposed visualization technique, the flow fields can be observed for different ranges of behavior.

3.2. Photographs

The cases shown in Figs. 4 to 7 are typical photographs that correspond to different bubble sizes. All the experiments were performed in water. The addition of tracers can, in some cases, modify the surface properties of the gas-liquid interface. The tracers were thoroughly washed with pure water prior to their addition to the test fluid. To verify that the effect of the tracers was minor, an additional series of measurements to determine the terminal velocity of the bubbles was carried out. The results were very similar to those presented in Fig. 8, which were performed without tracer particles. Hence, we are confident that the tracer "contamination" does not affect the results significantly.

In all the photographs both the bubble shape and the motion of the fluid are captured. The bubble images corresponds to the discrete instants at which the strobe light illuminated the bubble surface. The fluid streak lines depict the motion of the fluid particles for the time that the camera diaphragm remained opened. The bubble trajectory also results from the open diaphragm time. It must be noted that, on the photographs, due to the nature of the technique, the fluid streak lines may appear to occur *upstream* of the bubble image.

Fig. 4 shows the case of a 1.17 mm bubble. The trajectory of the bubble can be observed at the center of the photograph. This line image results from the reflection of the laser light on the gas-liquid interfase of the bubble. Clearly, for a bubble of this size the trajectory is rectilinear. The velocity field can be observed at the bottom of the photograph. Both the particles upstream and downstream of the bubble move upwards. This is a characteristic of the flow around an object that 'slides' through the fluid. It is, hence, similar to that predicted from an inviscid model. For the chosen flashing frequency, the

bubble appeared twice in the photo plate. For this case the position of the bubble has been highlighted. In the original set of photos the velocity field appears colored in red, while bubble appears in a blue tone. For publication purposes, the images are presented in a grey scale format. Original images can be obtained from the authors.

The Reynolds and Weber numbers for all cases are shown on the figures' captions. The values of the physical properties needed to calculate these numbers were obtained from tables ($\rho_f = 1000\,\mathrm{kg/m}^3, \mu_f = 0.001\,\mathrm{Pa\,s}, \sigma = 0.07\,\mathrm{N/m}$).

Figure 5 shows the motion of a 1.47 mm bubble. The velocity field does not appear to deviate largely from a potential flow prediction; however, a small amplitude oscillation of trajectory can be observed. For the case shown, the bubble velocity has not reached the value at which the inflection point is observed. Hence, the beginning of the bubble trajectory instability manifests itself before the flow around the bubble separates. The bubble shape and position are, in this case, clearly observed in the bottom end of the plate. The bubble image appears only once for this case.

For larger bubbles the shape of the velocity field changes drastically. Figures 6 and 7 show bubbles for sizes larger than that at which the inflection of the velocity curve occurs. Clearly, the velocity field is much more agitated. It is evident from the photographs that vortices have detached from the surface of the bubble. The structure that is observed is similar to the so-called Karman vortex street. In Fig. 6 the bubble is observed in several locations and the vortex detachment can be seen to alternate from left to right. In Fig. 8, the bubble images is captured only once, at the bottom of the photograph. Again, vortical structures can be observed to appear alternatively on the left and right to the bubble main trajectory. The flow disturbance is larger as the bubble size increases.

4. Summary and conclusions

The visualization technique presented in this article was used to analyze the nature of the flow around Nitrogen bubbles rising in clean water.

Based on the observations presented in this study, it can be argued that the appearance of the trajectory instability and the velocity-size curve inflection point are directly related to the appearance of detached vortices from the rear of the bubble (transition to unsteady flow). We can also conclude that the vortex detachment is not the only mechanism responsible from the appearance of the trajectory instability. Our observations are in accordance to other investigations.

We consider, on the other hand, that the reason behind to appearance of the inflection point in the bubble velocity curve results from the detachment of vortices. Since these fluid structures transport a considerable amount of energy away from the gas-liquid interfase, the bubble terminal velocity cannot increase in the same manner as the case in which vortices remain attached to the surface.

Modern velocimetry techniques, like particle image velocimetry (PIV), could be used to obtain quantitative measurements of the flow around bubbles. We plan to continue our investigation in this direction to further improve our understanding of the motion of a bubbles in a liquid.

Acknowledgements

∗ To whom correspondence should be addressed

1. G.B. Wallis, *One-dimensional two-phase flow*, (McGraw-Hill, 1969).

2. M.C. Roco, S. Rogers, S. Plasynski, *Proceedings of the NSF-DOE Workshop on Flow of Particulates and Fluids*, Washington, D.C., (National Science Foundation, 1990).

3. R. Zenit, D.L. Koch and A.S. Sangani, *J. Fluid Mech.* **429** (2001) 307-342.

4. R. Clift, J.R. Grace and M.E. Weber, *Bubbles, Drops, and Particles* (Academic Press, 1978).

5. P.C Duineveld, *J.Fluid Mech.* **292** (1995) 325.

6. M. Wu and M. Gharib, *Phys. Fluids* **14** (2002) L49.

7. G. Mougin and J. Magnaudet, *Phys. Rev. Lett.* **88** (2002) 014502.

8. D.W. Moore, *J. Fluid Mech.* **23** (1965) 749.

9. E. Kelley and M. Wu, *Phys. Rev. Lett.* **79** (1997) 1265.